4626 *Biochemistry* **2009,** *48,* 4626–4632
DOI:10.1021/bi900246h

BIOCHEMISTRY
including biophysical chemistry & molecular biology
Article

Heterochromatinization as a Potential Mechanism of Nickel-Induced Carcinogenesis[†]

Thomas P. Ellen,[‡] Thomas Kluz,[‡] Mark E. Harder,[§] Judy Xiong,[‡] and Max Costa*[,‡]

[‡]*Department of Environmental Medicine, New York University School of Medicine, 550 First Avenue, New York, New York 10016, and* [§]*Department of Biochemistry and Biophysics, Oregon State University, Corvallis, Oregon 97330*

Received February 14, 2009; Revised Manuscript Received April 1, 2009

ABSTRACT: Epigenetics refers to heritable patterns of gene expression that do not depend on alterations of the genomic DNA sequence. Nickel compounds have demonstrated carcinogenicity without any associated mutagenesis, suggesting that its mechanism of carcinogenesis is epigenetic in nature. One such potential mechanism is the heterochromatinization of chromatin within a region of the genome containing a gene sequence, inhibiting any further molecular interactions with that underlying gene sequence and effectively inactivating that gene. We report here the observation, by atomic force microscopy and circular dichroism spectropolarimetry, that nickel ion (Ni^{2+}) condenses chromatin to a greater extent than the natural divalent cation of the cell, magnesium ion (Mg^{2+}). In addition, we use a model experimental system that incorporates a transgene, the bacterial xanthine guanine phosphoribosyl transferase gene (*gpt*), differentially near, and far from, a heterochromatic region of the genome, in two cell lines, the Chinese hamster V79-derived G12 and G10 cells, respectively, to demonstrate by a DNase I protection assay that nickel treatement protects the *gpt* gene sequence from DNase I exonuclease digestion in the G12 cells, but not in the G10 cells. We conclude that condensation of chromatin by nickel is a potential mechanism of nickel-mediated gene regulation.

Chromatin is the natural state of protein-associated DNA in all eukaryotes. It is a dynamic polymer of subunits called nucleosomes. The nucleosome subunit consists of approximately 146 bp of DNA wrapped around an octamer of histone proteins. The histone octamer is made up histone H2A, H2B, H3, and H4 (two copies of each). The DNA makes one and one- half turns around the octamer, with the entry and exit points of the DNA at opposite sides of the disk-shaped histone octameric complex. This complex of 146 bp and the octamer of histones is known as the nucleosome core particle. In chromatin, the exiting and entering DNA duplex strands of this nucleosome core particle extend to the next nucleosome core particles on either side of it. The intervening DNA connecting each pair of nucleosomes is termed the linker DNA. The lengths of these intervening DNA duplex strands vary from species to species and from tissue type to tissues type, as well as from one stretch between two nucleosomes to another. Linker DNA length ranges from a minimum of 25 bp to upward of 100 bp, averaging approximately 50−60 bp (*1*). A fifth histone type, the linker histone (H1), binds to the linker DNA with a stoichiometry of one H1 to one nucleosome. The complex of the core particle (the histone octamer and 146 bp of DNA) with the additional 25 bp of DNA and the H1 molecule is called the chromatosome.

Chromatin exists in two states, corresponding to two structural forms, euchromatin and heterochromatin. Euchromatin structure has been characterized as "beads on a string". The DNA traces a random path punctuated by nucleosomes that appear as beads, or round protrusions, along the path of the stringlike DNA duplex. Heterochromatin is characterized as a thick fiber, with a diameter 2−3 times that of the "beads" of euchromatin, and appears to be much more rigid and less flexible than the beads on a string characterization of euchromatin (*2*). All physical data to date show that heterochromatin is much more irregular in shape and inconsistent in form than it would be if it were a simple rodlike fiber (*3*).

While the genome has been subdivided on the basis of the structural parameters of condensation and decondensation, the dynamics of chromatin are a functional phenomenon: euchromatin contains most of the transcriptionally active gene sequences, including, by and large, most of the unique DNA sequences of the genome, and these euchromatic regions decondense as the cell exits mitosis; heterochromatin, on the other hand, is made up of highly repetitive sequences of satellite DNA with a relatively small number of transcriptionally active genes interspersed. It is the program of heterochromatinization, whereby condensation spreads outward in cis, in response to epigenetic signaling events, that gives rise to the term "facultative heterochromatin", as distinguished from "constitutive heterochromatin", which applies to chromosomal regions that apparently

[†]This work was supported by Grants ES014454, ES005512, and ES000260 from the National Institute of Environmental Health Sciences (NIEHS) and Grant CA16087 from the National Cancer Institute (to M.C.) and Training Grants 5 T32 ES07324-08 and T32 NIEHS 007267-16 (to T.P.E.).

*To whom correspondence should be addressed: Department of Environmental Medicine, New York University School of Medicine, 550 First Ave., New York, NY 10016. Telephone: (845) 731-3515. Fax: (845) 351-2118. E-mail: costam@env.med.nyu.edu.

 Published on Web 4/1/2009

remain condensed in all cell types and at all stages of differentiation (*4*). The epigenetic signals mentioned here are the DNA methylations and histone modifications that in this context can result in a stably inherited gene silencing.

Our interest here with regard to heterochromatin lies in the capacity of the transition metal, nickel, to inactivate transcription of genes by inducing DNA methylation and chromatin compaction (*5*). Upon engulfment of a gene by the spreading of nearby heterochromatin, the gene is heritably silenced. Nickel-induced genotoxic effects such as DNA strand breaks, DNA−protein cross-links, and generation of reactive oxygen species (ROS) usually occur in heterochromatic DNA, which is not genetically active, and thus, this genotoxicity has little mutagenic consequence (*6*). This squares with evidence that nickel compounds are carcinogenic yet show no mutagenicity in mammalian cell assays. It is well established that chromosomally integrated transgenes in transfected cell lines and transgenic animals are susceptible to inactivation by changes in chromatin structure, thus revealing that chromatin structural change is a potential mechanism of transcriptional regulation (*7*−*9*).

Our laboratory has previously reported findings that nickel induces DNA hypermethylation, turning off a senescence gene during the course of nickel-induced transformation of Chinese hamster embryo cells (*10*, *11*). The mechanism by which nickel might be expected to stimulate DNA methylation was puzzling to us at that time. However, in studies using two differential cell lines, one (G12) in which a reporter gene (*gpt*) was inserted proximal to a heterochromatic region of chromosome 1 and the other (G10) in which the reporter gene was placed far from any heterochromatic region of chromosome 6, only the gene placed in, or near, the context of heterochromatin (G12) was down-regulated in response to nickel exposure. From these studies, we postulated a model of how nickel exerts its effects on the transcription of genes near heterochromatin (Figure 1) (*5*, *6*, *12*).

We propose that inactivation of transcription of a gene can be caused by nickel-induced chromatin condensation at euchromatin−heterochromatin junctions: the gene becomes incorporated into regions of spreading heterochromatin, and these conditions may also favor the methylation of the DNA within this newly condensed chromatin. This would also provide an explanation of nickel's carcinogenic properties in the absence of mutagenicity. The gene is engulfed by the newly condensed heterochromatin. Condensation could somehow signal DNA methylation of CpG islands. At replication, this methylation state would be inherited, an example of epigenetic inheritance. We hypothesize that DNA methylation takes place after chromatin condensation. We have not verified this experimentally, but *if* methylation occurs, then DNA methylation would be passed on to the next generation by the normal mechanism of DNA methylation inheritance. That mechanism has not been definitively demonstrated, and we do not pretend to know it. It has been suggested voluminously in the literature that the inheritance of cellular DNA methylation patterns is based on a CpG island-specific methylase that operates on newly replicated hemimethylated DNA (*13*).

Here, we have performed physical and chemical assays that demonstrate nickel's potential ability to inactivate genes by altering chromatin structure.

EXPERIMENTAL PROCEDURES

Preparation of Histone Octamers. Purified trimmed nucleosome monomers were prepared from chicken erythrocytes

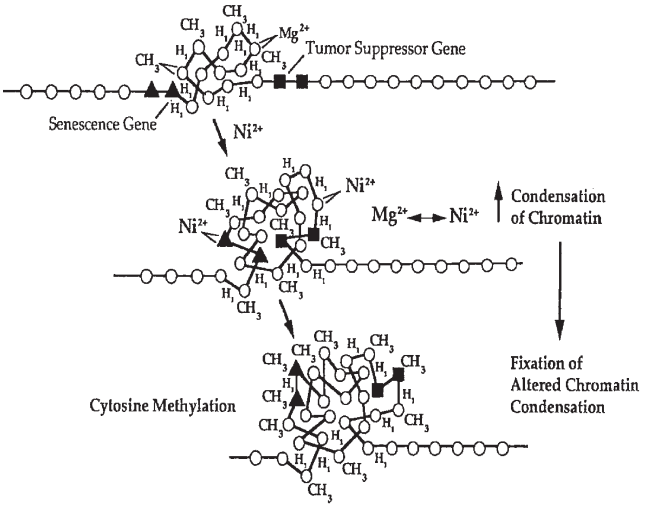

FIGURE 1: Model for transcriptional inactivation by Ni^{2+}. Molecular scheme for the enhanced chromatin condensation and subsequent DNA methylation induced by carcinogenic ionic nickel in cells. The gene silencing model shows how nickel-induced increases in heterochromatin condensation and hypermethylation may cause inherited inactivation of critical tumor suppressor or senescence genes. Cancer-relevant genes, such as tumor suppressor genes (squares) and senescence genes (triangles), may become incorporated into heterochromatin that is seeded by nickel-induced DNA condensation (middle panel) and stabilized by subsequent DNA methylation (bottom panel).

as described in detail (method II) by Yager et al. (*14*) and used as the source of histone octamers. Briefly, nuclei were prepared from 200 mL of chicken erythrocytes before being washed three times by centrifugation at 1464*g* for 5 min at 4 °C in 25 volumes of buffer A [0.34 M sucrose, 15 mM Tris, 60 mM KCl, 15 mM NaCl, 0.5 mM spermidine, 0.15 mM spermine, 2.5 mM EDTA, and 0.5 mM EGTA (pH 7.5)] containing 0.1 mM proteinase inhibitor phenylmethanesulfonyl fluoride (PMSF). The pelleted erythrocytes were lysed by repeated resuspension and centrifugation with the same buffer, but containing 0.5% Nonidet P-40. The nuclei were digested for 5 min at 37 °C with micrococcal nuclease (30 units/mg of DNA). The digestion was stopped by addition of EDTA and reduction of the temperature to 0 °C. The nuclei were washed and pelleted with a 20 min, 6800*g* centrifugation. The chromatin-containing pellet was resuspended in 10 mM Tris-HCl, 0.25 mM EDTA, and 0.35 M NaCl (pH 8.0), and the linker histones, H1/H5, were removed by incubation of the chromatin with 30 mg/mL carboxymethyl-Sephadex with stirring for 3 h at 4 °C. The cation-exchange resin was removed by centrifugation at 8000*g* for 30 min at 4 °C. Supernatant was dialyzed against TE [10 mM Tris (pH 7.8), 0.25 mM EDTA, and 0.1 mM PMSF] overnight at 4 °C, and again the next morning in fresh buffer for 2 h. (The resin is thrown out unless the linker histone is to be purified.)

Very briefly, a second micrococcal nuclease digestion was performed, followed by removal of the DNA by passing the sample through a hydroxylapatite (Bio-Rad, Hercules, CA) chromatography column equilibrated with the buffer described by Simon and Felsenfeld (*15*). Elution fractions were monitored by Laemmli (6%/15%) SDS−PAGE (*16*) and peak fractions pooled. The histone octamer concentration was determined by measurements of A_{230} (*17*).

Preparation of Template DNA. The DNA template $207\text{-}12_{601}$ consists of 12 tandem head-to-tail repeats of a 207 bp sequence derived from the selection studies of Lowary and

Widom (*18*). The 207-12_{601} DNA was cloned into pUC19 to produce plasmid pSG601 (a kind gift from S. Grigoryev), transformed, and propagated in DH5α cells. The 207-12_{601} tandem array was excised by XbaI/HindIII double restriction digests and isolated by gel filtration through a Sephacryl S-1000 column, eluting from TE [10 mM Tris-HCl (pH 7.8) and 0.25 mM EDTA].

Reconstitution of Nucleosomal Arrays. Nucleosomal arrays were reconstituted from chicken erythrocyte histone octamers and template 207-12_{601} DNA by salt gradient dialysis (*19*) as described previously (*20*).

Circular Dichroism (CD) Spectropolarimetry. CD was measured at room temperature on a Jasco J-720 spectropolarimeter (Jasco, Inc.). Spectra from 320 to 200 nm were recorded from the room-temperature samples. Ellipticities were averaged for 1 s in 1 nm steps with a 2 nm bandwidth. Scans for each sample were repeated 10 times and averaged.

Atomic Force Microscopy (AFM). Liquid samples (1 μL) were loaded onto mica discs and dried in a covered glass container at room temperature. Mica discs were freshly peeled to eliminate foreign particle background for each sample. The samples were scanned topographically by AFM in noncontact mode using a silicon ultralever tip (model MPP-11123) (Veeco Instruments, Santa Barbara, CA). Samples were characterized and sized by scanning at least four randomly selected fields on each substrate. For quality control, a 5 μm calibration grating with 100 nm × 100 nm pits was scanned periodically over the duration of the experiments to ensure image integrity. The surface scan data were processed and analyzed using Proscan version 1.9 image software (Veeco Instruments).

DNase I Protection Assay. The G10 and G12 cells were cultured in F12 medium (Life Technologies, Carlsbad, CA) supplemented with 1× HAT, 5% FBS, and 1% penicillin-streptomycin, at 37 °C in a humid 5% CO_2 atmosphere for 48 h. Twenty-four hours before the start of isolation of nuclei, medium was replaced with fresh F12 medium without HAT.

Nuclei were isolated using Sigma's Nuclei Pure Prep Nuclei Isolation kit, according to the manufacturer's protocol. Metal treatments were conducted on ice at a rate of 10^6 nuclei/mL for 75 min in nuclei storage buffer (Sigma, St. Louis, MO). Nuclei were then centrifuged at 600*g* and 4 °C for 15 min and washed once with nuclei storage buffer.

Treated nuclei were resuspended in DNase I buffer [10 mM Tris-HCl (pH 7.4), 10 mM NaCl, 3 mM $MgCl_2$, and 100 μM $CaCl_2$] at a rate of 10^6 nuclei/mL; 195 μL of nuclei was added to each tube containing 5 μL of DNase I (Roche, Indianapolis, IN). DNase I digestions were performed on ice for 20 min; 200 μL of stop solution [1% sodium dodecyl sulfate, 0.3 M NaCl, 50 mM Tris-HCl (pH 8.0), 50 mM ethylenediaminetetraacetic acid, and 20 μg of RNase A] was then added to each sample, and samples were mixed and placed on ice for 30 min to stop the reaction. Ten microliters of a 20 mg/mL solution of Proteinase K was then added to each tube, and the tubes were mixed and incubated at 65 °C for 18 h.

Samples were extracted with phenol and chloroform and precipitated with 2.5 volumes of 100% ethanol in the presence of Polyacryl carrier (Molecular Research Center, Cincinnati, OH). Visible pellets were washed with 70% ethanol, air-dried, and resuspended in 10 mM Tris-HCl (pH 8.0).

The digested DNAs were subjected to PCR using a specific *gpt* PCR primer set (5′TATTGTAACCCGCCTGAAGTTAAA3′ and 5′AACACTTTTTAAGCCGTAGATAAA3′), annealing at 55 °C. The primers encompass a 581 bp DNA sequence containing the coding region of the *gpt* gene.

RESULTS

A Model Oligonucleosome. We reconstituted oligonucleosomal tandem arrays, as described in Experimental Procedures, that were of homogeneous constitution and with subunits (the nucleosomes) that were positioned along the 12-mer tandem array with perfect regularity. We did this by using the 207-12_{601} DNA based on the Widom 601 DNA which had been cloned to make a 12-mer repeat of the 207 bp DNA sequence (*21*). This DNA positions one histone octamer uniquely and with high affinity at each of the 207 bp repeats. Sedimentation velocity analysis verified that these nucleosomal arrays were homogeneous in structure (data not shown), with one histone octamer bound per 207 bp tandem repeat of the 207-12_{601} DNA, and 12 core octamers for each 12-mer DNA 207 bp repeat.

Figure 2 shows an atomic force microscopic image of one of these reconstituted oligonucleosomes in an extended form in the absence of divalent cation and with very little salt (10 mM Tris-HCl). It is well-known and it has been well documented that salt, either monovalent (NaCl) or divalent (for example, $MgCl_2$), condenses the chromatin structure in solution (*22*−*24*). The data show that the ionic environment has a great influence on the extent of condensation from the 10 nm polynucleosome chain to the so-called "30 nm fiber" of condensed higher-order chromatin structure. Although the in vivo state of chromatin is influenced by a mixture of both mono- and divalent cations, divalent cations perturb chromatin structure at concentrations that are nearly 3 orders of magnitude lower than those of monovalent cations. When considering the following biophysical data presented, it would be helpful to keep in mind that the concentrations of mono- and divalent cations in nucleo are sufficiently high to maintain most of the chromatin in a highly condensed state. Both monovalent and divalent cations are capable of holding the chromatin fiber at comparable levels of condensation, but at concentrations that are orders of magnitude lower in the case of divalent cations, indicating that condensation of the fiber is not simply due to changes in ionic strength. The special interaction of divalent cations with negative charges of the DNA phosphates is probably what leads to their particular effectiveness in the compaction process. Also, because the 30 nm fiber is a functional as well as a physical entity, it is probably most appropriate to consider it a structurally heterogeneous and dynamically transmuting complex at any given instant.

Condensation of Oligonucleosomes in the Presence of Divalent Cations. Reconstituted oligonucleosome samples were exposed to various concentrations of the divalent cation magnesium in the form of the soluble $MgCl_2$, and CD measurements were taken to examine the organization of DNA in these oligonucleosomal preparations. Figure 3A shows that there is significant difference between the CD spectra of oligonucleosomes in the presence and absence of the divalent cation. The maximum molar ellipticity value at 272 nm decreases from ~6000 for oligonucleosomes in the absence of divalent cation to 5000 in the presence of 0.6 mM Mg^{2+}. As shown in Figure 3B, the decrease in the maximum molar ellipticity value at 272 nm is significantly greater in the presence of equivalent amounts (0.6 mM) of Ni^{2+}, reduced to ~3000. These concentrations of divalent ion were those that caused the greatest increment of change in molar ellipticities.

Of particular interest is the formation of two well-resolved peaks at 282 and 272 nm in the positive band which are absent in the samples that have not been exposed to divalent cation (Figure 3A,B, compare broken to solid lines in each). These are considered a characteristic feature of the intranucleosomal DNA−histone interactions of the core particle that are absent in the looser configuration of core particles in the beads on a string structure (*25*−*27*). Note that this characteristic appears much more clearly in the case of nickel-exposed oligonucleosomes than in that of magnesium-exposed ones. This is a clear indication of high-affinity molecular interactions characteristic of DNA−histone molecule binding in the context of higher-order chromatin structure, observed in nickel-treated oligonucleosomes but not observed as significantly in magnesium-treated oligomers.

This distinction is corroborated by the atomic force microscopic images of these same samples, as seen in Figure 4, unfixed and mounted, without vacuum, in air. Figure 4B shows oligonucleosomal arrays in the presence of magnesium, and Figure 4C shows the arrays in the presence of nickel. While the magnesium-exposed oligonucleosomes in Figure 4B exhibit significant compaction, the nickel-exposed oligonucleosomes in Figure 4C are still more condensed, and there are fewer small beadlike structures, indicating that few nucleosomes have escaped the condensation process. We tested with various concentrations of divalent cations, but the concentrations of divalent cation as shown here were those that had the greatest, most significant and dramatic effects observed.

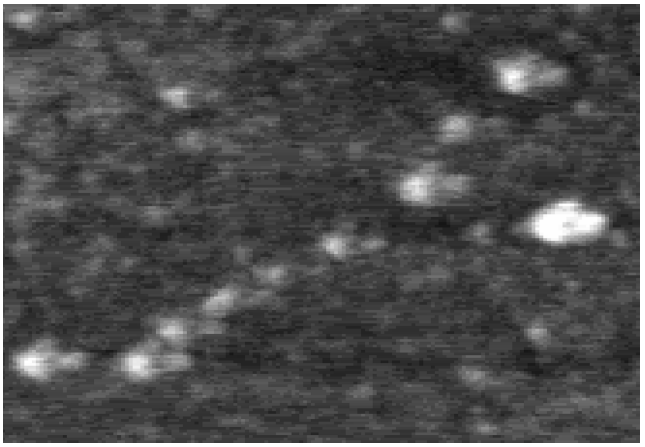

FIGURE 2: Atomic force microscopic image of an unfixed oligonucleosomal array in TE buffer [10 mM Tris-HCl (pH 8.0) and 0.1 mM EDTA].

Nickel Induces Greater Protection from DNase I Cleavage Than either Magnesium or Cobalt. We have previously reported that nickel yields very high levels of 6-thioguanine (6TG) resistance at the bacterial xanthine guanine phosphoribosyl transferase (GPT) locus (*gpt*) in Chinese hamster V79-derived G12 cells (*28*, *29*). The G12 cell line carries a single copy of *gpt*, the gene for a bacterial nucleotide salvage enzyme that is functionally analogous to the endogenous mammalian hypoxanthine phosphoribosyl transferase (HPRT) gene (*hprt*). Inactivation of xanthine guanine phosphoribosyl transferase (gpt^-) is selected by resistance to 6TG, and gene reactivation (gpt^+) is selected by resistance to a mixture of 100 μM hypoxanthine, 1 μM aminopterin, and 100 μM thymidine (HAT) (*30*, *31*).

In later work, we compared the Chinese hamster V79-derived G12 cell line, whose transgenic *gpt* plasmid-borne gene has been stably inserted into a site on chromosome 1 near an interstitial subtelomeric band of dense constitutive heterochromatin identified in V79 karyotypes (*32*), with the Chinese hamster V79-derived G10 cell line, whose transgenic *gpt* plasmid-borne gene appears to have been inserted, in contrast, in a euchromatic region of chromosome 6 (*5*). Thus, the G12 transgene is likely to lie within condensed heterochromatin, while the G10 transgenic *gpt* is far from any condensed chromatin and likely to remain accessible to DNA processes such as transcription, DNA repair, and replication. The results of this comparison led to our proposal that it was the chromosomal integration of the G12's transgene near the heterochromatin of chromosome 1 and the lack of heterochromatinization at the euchromatic integration site of the *gpt* transgene in the G10 cell line that explain the inactivation of *gpt* in G12 and its activation in G10. DNase I protection assays, often used as an indicator of chromatin

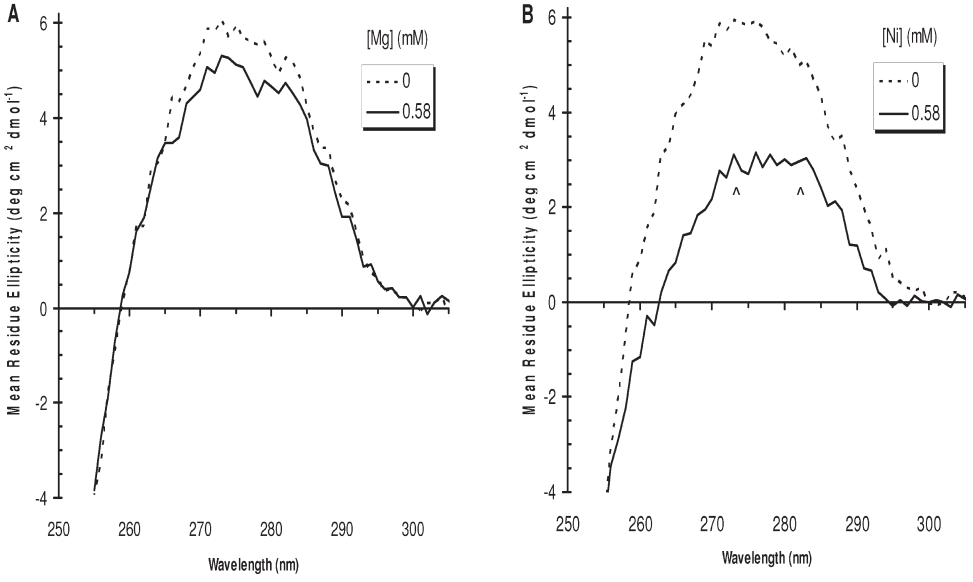

FIGURE 3: CD spectral difference for dodecanucleosomes in the absence or presence of divalent cations. Ions reduce the peak signal at 272 nm. The dashed lines are the CD spectra in the absence and solid lines those in the presence of divalent cation, at the indicated concentrations. Arrowheads in panel B show the two closely spaced peaks at 272 and 282 nm.

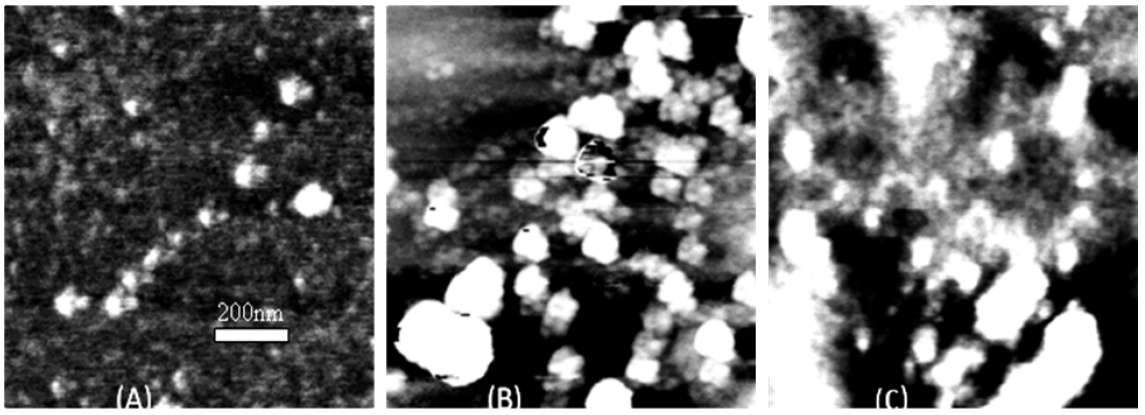

FIGURE 4: Atomic force microscopy (AFM) images of unfixed dodecanucleosomal fibers in TE buffer [10 mM Tris-HCl (pH 8.0) and 0.1 mM EDTA]: (A) no divalent cation, (B) treated with 1.0 mM Mg^{2+}, and (C) treated with 1.0 mM Ni^{2+}. For either divalent ion, 1.0 mM was the concentration at which the greatest, most significant and dramatic effects were observed.

condensation state, showed resistance of the heterochromatic region of the *gpt* gene in G12 to DNase I, while that of the G10 cell line gave no such resistance to DNase I cleavage.

Therefore, we wished to reevaluate the extent of DNase I protection of G12 and G10 cell line-derived chromatin induced by nickel and compare the protection expected to be induced by nickel with that of other divalent cations, namely, magnesium and cobalt. Figure 5 is the result of a DNase I footprint assay for nickel, magnesium, and cobalt. Although nickel-treated chromatin from the G12 cell line was entirely refractory to DNase I cleavage, magnesium showed weak protection at a concentration 20 times that of the nickel and cobalt showed no indication of protecting G12 cell line-derived chromatin from cleavage. As expected, G10 cell line-derived chromatin was cleaved whether it was untreated or treated with nickel, cobalt, or magnesium.

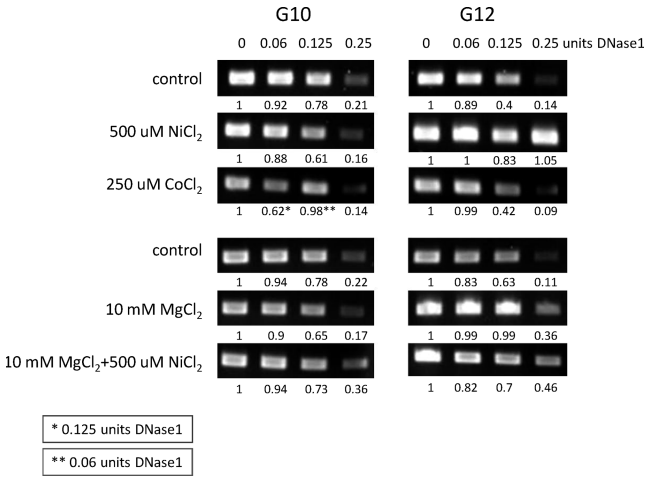

FIGURE 5: GPT DNase I protection assay. Nickel-induced DNase I protection of chromatin in comparison to that with magnesium and cobalt. DNase I-treated samples were extracted with phenol and chloroform, precipitated, washed, and resuspended in 10 mM Tris-HCl (pH 8.0), and the resulting DNA was amplified by PCR, as described in Experimental Procedures. Shown is a 1.0% agarose gel of amplified DNA. The number below each DNA band is the relative amount of DNA (compared to control DNA that was treated with no DNase I and normalized to "1") that had remained after (that is, the relative amount that had been protected from) DNase I digestion. As shown, 500 μM $NiCl_2$ treatment of G12, but not G10, nuclei resulted in DNA that was protected from DNase I digestion significantly more than DNA treated with either cobalt, magnesium, or a mixture of both nickel and magnesium. This is taken to be an indication that the chromatin of G12 cells was heterochromatinized in the region of the *gpt* transgene by nickel treatment. Chromatin of G10-derived cells showed no sign of heterochromatinization under such conditions, and magnesium and cobalt showed little or no effect in G12- or G10-derived chromatin exposed to the highest DNase I concentration.

DISCUSSION

Our previously reported findings that nickel-induced inactivation of gpt expression in a transgenic *gpt*+ G12 cell line occurs without mutagenesis or deletion of the transgene (*5*) led to our hypothesis that nickel silenced the gene by an epigenetic mechanism. In this work, we have shown that (1) nickel (Ni^{2+}) condenses a model chromatin and that the resulting higher-order structure is more compact than the same model chromatin treated with magnesium (Mg^{2+}), suggesting that nickel is a powerful competitor capable of displacing magnesium from a protein−DNA complex, and (2) when nickel exerts its effect on a chromatin region that contains an active gene, namely the transgene *gpt*, nickel prevents accessibility to that gene, thus changing the functional state of the underlying DNA epigenetically, since the sequence of the DNA has not changed. We observed that the model *gpt* transgene is regulated by nickel-induced condensation only when it is inserted in the region proximal to the dense, heterochromatic chromatin of chromosome 1 of V79-derived cell line G12 and is not thusly regulated when inserted in the euchromatic regions of chromosome 6 of V79-derived cell line G10. In combination with our previous report (*5*) that nickel induces DNA hypermethylation and thereby silences a gene during the course of nickel-induced transformation of Chinese hamster cells, we can now propose a potential epigenetic mechanism of nickel-induced carcinogenesis.

Interactions of nickel divalent cations (Ni^{2+}) with chromatin facilitate chromatin compaction, creating dense, heterochromatic regions which spread at either end or both ends of the chromatin fiber. Previously, we have shown that the *gpt* gene in G12 cells is regulated by epigenetic processes, including chromatin condensation and DNA methylation of CpG islands within the *gpt* transgene (*5*), and that these processes were reversible. Thus, it is possible that heterochromatinization is followed by DNA methylation, and the resulting silencing of the underlying gene is likely inherited by subsequent generations through this epigenetic mechanism. If these nascent silenced chromatin regions contained tumor suppressor or senescence-related genes, the outcome might be cell transformation, tumor progression, and,

ultimately, oncogenesis. In fact, this epigenetic mechanism of nickel carcinogenesis may be more prominent than any other proposed to date.

There is substantial evidence that nickel interacts preferentially with the heterochromatic regions of chromosomes (*33*), and the selective interactions of nickel with heterochromatin may explain why nickel compounds are not generally mutagenic. Nickel ion (Ni^{2+}) was shown here by CD spectropolarimetry and atomic force microscopy (AFM) to increase the level of chromatin condensation much more effectively than Mg^{2+}. This is in agreement with results obtained by other laboratories using other biophysical and hydrodynamic techniques (*23*). In previous studies (*5*), we have shown that DNA hypermethylation was associated with decreased DNase I sensitivity, and in those studies, the silencing of the *gpt* gene was readily reversible by the addition of azacytidine, a reagent which induces hypomethylation. It is clear from this earlier work that nickel can induce hypermethylation, and we propose that both heterochromatinization and DNA hypermethylation are potential mechanistic processes in nickel carcinogenesis. We believe that DNA hypermethylation has the capacity to stabilize the nascent spreading of chromatin condensation in cis that can be induced by nickel ion's displacement of Mg^{2+} in heterochromatic complexes, as represented in Figure 1, with the potential to perpetuate a heritable epigenetic state through subsequent generations.

Here we have shown supporting evidence that nickel interacts preferentially with heterochromatin rather than euchromatin, since nickel exposure increased DNase I protection in the heterochromatic regions of the V79-derived G12 cell line, while exhibiting no protective effect in euchromatic regions of the V79-derived G10 cell line. This is not surprising as nickel ions bind proteins with much greater affinity than they do DNA. For example, the binding constant of nickel for DNA is $K = 7.3 \times 10^2\ M^{-1}$, while typical binding constants of nickel for amino acids such as cysteine and histidine are 4.37×10^9 and $1.9 \times 10^9\ M^{-1}$, respectively (*33*). It has been clearly shown that there is a structural condensation of chromatin induced by nickel and that nickel condensed chromatin more that magnesium did. We believe it is more likely that chromatin condensation is followed by DNA methylation than vice versa because nickel ions should have greater avidity, if not affinity, for chromatin than for specific DNA methylase enzymes.

The molecular interactions shown here between divalent nickel ion (Ni^{2+}) and a defined molecular model of chromatin and the structural contribution of that interaction to a potential nickel-induced epigenetic mechanism of gene regulation shown here in the context of chromatin associated with a specific functional transgene (*gpt*) support a model of a potential epigenetic mechanism by which chromatin exposure to nickel leads to carcinogenesis through a structural modulation of chromatin, such as heterochromatinization. This may be one of the most prominent mechanisms of nickel-induced carcinogenesis.

ACKNOWLEDGMENT

We thank Dr. Michael Schimmerlik (Oregon State University) for the use of the CD spectropolarimeter and Sergei Grigoryev (Pennsylvania State University, University Park, PA) for the kind gift of the pSG601 DNA.

REFERENCES

1. Van Holde, K. E. (1989) *Chromatin*, Springer-Verlag, New York.
2. Thoma, F., Koller, T., and Klug, A. (1979) Involvement of histone H1 in the organization of the nucleosome and of the salt-dependent superstructures of chromatin. *J. Cell Biol. 83*, 403–427.
3. Van Holde, K. E., and Zlatanova, J. (2007) Chromatin fiber structure: Where is the problem now?. *Semin. Cell Dev. Biol. 18*, 651–658.
4. Eissenberg, J. C., and Elgin, S. C. R. (2005) Heterochromatin and euchromatin, *Encyclopedia of Life Sciences*, pp 1−7, John Wiley & Sons, New York..
5. Lee, Y.-W., Klein, C. B., Kargacin, B., Salnikow, K., Kitahara, J., Dowjat, K., Zhitkovich, A., Christie, N. T., and Costa, M. (1995) Carcinogenic nickel silences gene expression by chromatin condensation and DNA methylation: A new model for epigenetic carcinogens. *Mol. Cell. Biol. 15*, 2547–2557.
6. Costa, M. (1995) Inactivation of critical cancer-related genes by nickel-induced DNA hypermethylation and increased chromatin condensation: A new model for epigenetic carcinogenesis. In *Genetic Response to Metals* (Sarkar, B., Ed.) Chapter 4, pp 53−68, Marcel Dekker, Inc., New York..
7. Al-Shawi, R., Kinnaird, J., Burke, J., and Bishop, J. O. (1990) Expression of a foreign gene in a line of transgenic mice is modulated by a chromosomal position effect. *Mol. Cell. Biol. 10*, 1192–1198.
8. Davies, R. L., Fuhrer-Krusi, S., and Kucherlapati, R. S. (1982) Modulation of transfected gene expression mediated by changes in chromatin structure. *Cell 31*, 521–529.
9. Swain, J. L., Stewart, T. A., and Leder, P. (1987) Parental legacy determines methylation and expression of an autosomal transgene: A molecular mechanism for parental imprinting. *Cell 50*, 719–727.
10. Klein, C. B., Conway, K., Wang, X. W., Bhamra, R. K., Lin, X., Cohen, M. D., Annab, L., Barrett, J. C., and Costa, M. (1991) Senescence of nickel-transformed cells by an X chromosome: Possible epigenetic control. *Science 251*, 796–799.
11. Wang, X. W., Lin, X., Klein, C. B., Bhamra, R. K., Lee, Y.-W., and Costa, M. (1992) A conserved region in human and Chinese hamster X chromosomes can induce cellular senescence of nickel-transformed Chinese hamster cell lines. *Carcinogenesis 13*, 555–561.
12. Ellen, T. E., and Costa, M. (2009) Carcinogenic Inorganic Chemicals. In *Comprehensive Toxicology* (Roberts, R., and McQueen, C., Eds.) 2nd ed., Vol. *14*, Elsevier, Oxford, U.K..
13. Rountree, M., Bachman, K. E., Herman, J. G., and Baylin, S. B. (2001) DNA methylation, chromatin inheritance, and cancer. *Oncogene 20*, 3156–3165.
14. Yager, T. D., McMurray, C. T., and van Holde, K. E. (1989) Salt-induced release of DNA from nucleosome core particles. *Biochemistry 28*, 2271–2281.
15. Simon, R. H., and Felsenfeld, G. (1979) A new procedure for purifying histone pairs H2A + H2B and H3 + H4 from chromatin using hydroxylapatite. *Nucleic Acids Res. 6*, 689–696.
16. Laemmli, U. K. (1970) Cleavage of structural proteins during the assembly of the head of bacteriophageT4. *Nature 227*, 680–685.
17. Stein, A. (1979) DNA folding by histones: The kinetics of chromatin core particle reassembly and the interaction of nucleosomes with histones. *J. Mol. Biol. 130*, 103–134.
18. Lowary, P. T., and Widom, J. (1998) New DNA sequence rules for high affinity binding to histone octamer and sequence-directed nucleosome positioning. *J. Mol. Biol. 276*, 19–42.
19. Tatchell, K., and van Holde, K. E. (1977) Reconstitution of chromatin core particles. *Biochemistry 16*, 5295–5303.
20. Hansen, J. C., Ausio, J., Stanik, V. H., and van Holde, K. E. (1989) Homogeneous reconstituted oligonucleosomes, evidence for salt-dependent folding in the absence of histone H1. *Biochemistry 28*, 9129–9136.
21. Thastrom, A., Lowary, P. T., Widlund, H. R., Cao, H., Kubista, M., and Widom, J. (1999) Sequence motifs and free energies of selected natural and non-natural nucleosome positioning DNA sequences. *J. Mol. Biol. 288*, 213–229.
22. Ausio, J., Borochov, N., Seger, D., and Eisenberg, H. (1984) Interaction of chromatin with NaCl and $MgCl_2$: Solubility and binding studies, transition to and characterization of the higher-order structure. *J. Mol. Biol. 177*, 373–398.
23. Borochov, N., Ausio, J., and Eisenberg, H. (1984) Interaction and conformational changes of chromatin with divalent ions. *Nucleic Acids Res. 12*, 3089–3096.
24. Walker, P. R., Sikorska, M., and Whitfield, J. F. (1986) Chromatin structure: Nuclease digestion profiles reflect intermediate stages in the

folding of the 30-nm fiber rather than the existence of subunit beads. *J. Biol. Chem. 261*, 7044–7051.
25. De Murcia, G., Das, G. C., Erard, M., and Duane, M. (1978) Superstructure and CD spectrum as probes of chromatin integrity. *Nucleic Acids Res. 5*, 523–535.
26. Lawrence, J.-J., Chan, D. C. F., and Piette, L. H. (1976) Conformational state of DNA in chromatin subunits. Circular dichroism, melting, and ethidium bromide binding analysis. *Nucleic Acids Res. 3*, 2879–2893.
27. Stein, A., Bina-Stein, M., and Simpson, R. T. (1977) Crosslinked histone octamer as a model of the nucleosome core. *Proc. Natl. Acad. Sci. U.S.A. 74*, 2780–2784.
28. Kargacin, B., Klein, C. B., and Costa, M. (1993) Mutagenic responses of nickel oxides and nickel sulfides in Chinese hamster V79 cell lines at the xanthine-guanine phosphoribosyl transferase locus. *Mutat. Res. 300*, 63–72.
29. Lee, Y.-W., Pons, C., Tummolo, D. M., Klein, C. B., Rossman, T. G., and Christie, N. T. (1993) Mutagenicity of soluble and insoluble nickel compounds at the gpt locus in G12 Chinese hamster cells. *Environ. Mol. Mutagen. 21*, 365–371.
30. Klein, C. B., and Rossman, T. G. (1990) Transgenic Chinese hamster V79 cell lines which exhibit variable levels of gpt mutagenesis. *Environ. Mol. Mutagen. 16*, 1–12.
31. Klein, C. B., Su, L., Rossman, T. G., and Snow, E. T. (1994) Transgenic gpt+ V79 cell lines differ in their mutagenic response to clastogens. *Mutat. Res. 304*, 271–228.
32. Thacker, J. (1981) The chromosomes of a V79 Chinese hamster line and a mutant subline lacking HPRT activity. *Cytogenet. Cell Genet. 29*, 16–25.
33. Sen, P., Conway, K., and Costa, M. (1987) Comparison of the localization of chromosome damage induce by calcium chromate and nickel compounds. *Cancer Res. 47*, 2142–2147.